AMERICAN UNIVERSITY OF BEIRUT

NATURAL VENTILATION INDUCED BY TROMBE WALL USING BASEMENT AIR

by
MAZEN ISMAIL BADAWIYEH

A thesis
submitted in partial fulfillment of the requirements
for the degree of Master of Engineering
to the Department of Mechanical Engineering
of the Faculty of Engineering and Architecture
at the American University of Beirut

Beirut, Lebanon
September 2015

AMERICAN UNIVERSITY OF BEIRUT

NATURAL VENTILATION INDUCED BY TROMBE WALL USING BASEMENT AIR

by

MAZEN ISMAIL BADAWIYEH

Approved by:

Sept. 29, 2015

Dr. Nesreene Ghaddar, Professor — Advisor
Department of Mechanical Engineering

Sept. 29, 2015

Dr. Kamel Ghali, Professor — Co-Advisor
Mechanical Engineering

Sept. 29, 2015

Dr. Ghassan Chehab, Assistant Professor — Member of Committee
Civil and Environmental Engineering

Date of thesis defense: September 15, 2015

AMERICAN UNIVERSITY OF BEIRUT

THESIS, DISSERTATION, PROJECT RELEASE FORM

Student Name: Badawiyeh (Last) Mazen (First) Ismail (Middle)

● Master's Thesis ○ Master's Project ○ Doctoral Dissertation

[X] I authorize the American University of Beirut to: (a) reproduce hard or electronic copies of my thesis, dissertation, or project; (b) include such copies in the archives and digital repositories of the University; and (c) make freely available such copies to third parties for research or educational purposes.

[ ] I authorize the American University of Beirut, **three years after the date of submitting my thesis, dissertation, or project,** to: (a) reproduce hard or electronic copies of it; (b) include such copies in the archives and digital repositories of the University; and (c) make freely available such copies to third parties for research or educational purposes.

Signature Date Sept 29, 2015

This form is signed when submitting the thesis, dissertation, or project to the University Libraries

ACKNOWLEDGMENTS

First of all, I am extremely grateful and thankful to Almighty ALLAH for providing me with the ability, understanding and insight to complete this work.

I would like to thank my advisors Prof. Nesreene Ghaddar and Prof. Kamel Ghali for their dedicated help and support during work time at AUB and during Holidays and weekends. Their motivation was very essential to initiate and boost this work. Their guidance was very helpful for me to be able to complete the years spent on accomplishing my master's degree at AUB.

I would like to thank Dr. Ghassan Chehab for reviewing my thesis as a member of my thesis committee in a short notice.

I would like to acknowledge the support and help of all the staff and faculty members at the American University of Beirut.

I would like to extend my sincere appreciation and deepest gratitude to Prof. Ali Hammoud, Prof. Hisham Basha, Dr. Adnan Al Masri, and Mr. Mahmoud Rihabi who in one way or another have contributed in making this study possible.

I would also want to send my appreciation to all my friends and colleagues for their support throughout my research time. I would especially like to thank Riad Sawwan, Mohammad Kanaan, Mario El Hourani, Raghid Farhat, Mohammad Reda, Jad Hawi, Olfat Shibbo, Gihan Nakhleh, Nour Karaki, Mohamed Edelby, Mohamed Hanbali, Mohamad Knio, Hadi Chaar, Khaled Chaaban, Ghayass Tohme, Ameen Ghraizi, Mohammed Kassem, and Toufic Mansour.

Last but not least, I would like to express my heartfelt thanks to my family for their great patience and unconditioned love and support in the period during which this work was finalized. I would be nowhere near where I am today without their unceasing encouragement and support. I also owe a very special thanks to my mother who has always stood by me in times of need and to whom I owe my life for her constant love, moral support and blessings. Special thanks are due to my one and only loving brother who always strengthened my morale by standing by me in all situations.

AN ABSTRACT OF THE THESIS OF

Mazen Ismail Badawiyeh for Master of Engineering
Major: Applied Energy

Title: Natural Ventilation Induced by Trombe Wall using Basement Air

The aim of this work is to study the viability of utilizing natural ventilation using a Trombe wall drawing fresh air from underground basement floor for indoor thermal comfort in the dry desert climate. The fresh air is introduced at a low level to the basement by means of an earth tube. A numerical model was developed that integrated thermal models of the basement space and the occupied zone, and the Trombe wall to predict the indoor air temperature and comfort conditions and to evaluate the energy performance of the integrated system. The various sub-models were validated with published data in literature.

The model was applied to a case study to assess feasibility of depending on natural ventilation for comfort during the summer months in dwelling unit located in the inland plateau of Lebanon. The simulation results showed that a thermally comfortable indoor environment was attained for a large number of hours. During the sunshine hours, thermal comfort conditions were maintained for about 58.3% to 83.3% depending on the month of the year.

CONTENTS

ILLUSTRATIONS

Figure

Page

TABLES

Table Page

Dedication addressed

To my family and friends

CHAPTER 1

INTRODUCTION

With increased world population and human development, the energy demand of the buildings is forecasted to continue rising around the world in the nearing decades if measures are not strictly applied to reduce dependence on electrical energy (Xing et al. 2011; Ibn-Mohammed et al. 2013; IEA 2013). The residential sector is considered to be the third-largest major energy consumer in the world, accounting for 27% of the total energy consumption (Laustsen 2008). Hence, energy effectiveness should be enhanced by adopting policies to improve energy efficiency performance of building components such as windows and heating ventilation and air-conditioning (HVAC) systems for new and existing buildings (IEA 2013). On the other hand, relying on ventilation for cooling and heating purposes could be a viable option for reducing energy consumption in residential buildings.

Proper ventilation is a critical consideration for homes and buildings. Poor ventilation can cause a buildup in indoor air pollutants like dust, pollen, mold, and household chemicals. An efficient and reliable ventilation system works to remove polluted air while continuously introducing fresh, clean air. Thus, the primary purpose of ventilation is to provide acceptable indoor air quality and thermal comfort. Fresh air can be introduced indoors by natural ventilation, mechanical ventilation or by an hybrid combination of them.

Natural ventilation, relying on wind and thermal buoyancy as driving forces, is surely not a new phenomenon or invention. However, the use of a mechanical driving

force, i.e. fans, to drive the ventilation through a network of ducts has dominated over natural ventilation in the twentieth century (Kleiven 2003). Mechanical ventilation has offered a stable airflow, possibilities for air treatment (e.g. air conditioning) and allowed heat recovery but on the other hand, it constitutes a great share of the building's construction and running costs (Wigginton and Harris 2002) and it tends further to generate noise (both inside and outside of buildings) and is often difficult to clean and maintain. This, together with an increased awareness of the environmental consequences of a steadily increasing consumption of energy (Roodman and Lenssen 1995) has directed the focus on better building integrated and less energy consuming alternatives (Ford 2002).

In the literature, there were many studies reporting the savings on cooling energy that could be attained by using natural ventilation strategies as compared to identical buildings for which mechanical ventilation systems were used. The primary energy consumption of naturally ventilated office buildings in Denmark was compared with mechanical ventilation systems and it was reported that naturally ventilated buildings consumed 40 kWh/m^2 per year, whereas the mechanical systems consumption varied from 50 kWh/m^2 per year for variable air volume system to 90 kWh/m^2 per year for constant air volume system (Froland-Larson 2001). Moreover, studies conducted on the 23-story Liberty Tower of Meiji University in Tokyo showed that about 17% of energy consumption for cooling was saved by using the natural ventilation system (Schulz and Eicker 2013). Unfortunately, one of the main drawbacks of natural ventilation is that it depends on the outdoor conditions, which means that if the outside air temperature is high, then there would be no possibility of taking advantage of this system in this case however, it still be very useful in providing night ventilation.

Nonetheless, the use of natural, mechanical, or even hybrid (natural and mechanical) ventilation systems cannot always ensure thermal comfort conditions throughout the whole year. Additional systems are sometimes necessary to aid in providing acceptable thermal comfort year-round. One such system is the earth to air heat exchanger (EAHE) which has been found to be the most common technique being used by many researchers since the late 1970's and early 1980's in order to provide passive cooling (EERE 2009). This technique was implemented in an office building in Marburg in Germany (Voss et al. 2007; Spieler et al. 2000; Wagner et al. 2000), in a school in Italy (Grosso and Raimondo 2008), and in a hospital building in India (Badescu and Isvoranu 2011). Moreover, some researchers considered integrating the mechanical ventilation with earth to air heat exchanger to increase the effectiveness of ventilation during the day when the air temperature is high (Peretti et al. 2013). However, these techniques are expensive as they require excavation of high initial cost in addition to the fan cost. In this regard, there is a growing attention toward the application of more passive techniques that do not require the high initial cost and can be operated by solar energy such as: the Trombe wall and the solar chimney (Yuebin et al. 2013).

Trombe wall and solar chimney are relatively similar. They are passive building elements which rely on solar-induced buoyancy-driven convection. Numerous studies and researches have dealt with the heating performances of passive solar elements, but very little had been done to analyze their behavior in hot climatic conditions. Yaghoubi and Sabzevari (1987) have presented a study on the summer behavior of passive solar buildings in a hot arid region of Iran. Al-Motawakel et al. (1987) have considered thermal performances of direct gain and Trombe wall under

Yemeni conditions. Gan (1998) studied the ventilation of the Trombe wall using a CFD numerical analysis in the aim of using it for summer cooling. On the other hand, Yuebin et al. (2013) conducted a systematic study through three different experimental tests of an existing test facility of a coupled geothermal cooling system with an earth-to-air heat exchanger and a solar collector enhanced solar chimney in order to evaluate the performance of the system in summer, in terms of passive cooling capability, active cooling capability, and soil thermal capability. The results showed that the coupled geothermal system was feasible to provide cooling to the facility in natural operation mode free without using any electricity. Therefore, the solar chimney or the Trombe wall can replace the assisted fan thus reducing the initial and the operational costs but unfortunately, it still did not resolve the issue of expensive excavation.

In this study, it is proposed to utilize basement air to supply moderated ventilation air by means of a vertical earth tube. The temperature of the captured ambient air is dramatically dropped in view of the fact that basement acts as a cooling source since it is surrounded by the soil. Moreover, the moderated air from the basement is introduced by pressure difference to condition the living space using a Trombe wall that acts as an alternative to the fan. This wall generates the buoyancy force needed to draw the cooler air from the basement. Note that the solar radiation for the proposed system has a significant effect on the induced air mass flow rate.

The capability of utilizing natural ventilation in a typical dwelling unit with a basement, located in the inland plateau of Lebanon, was investigated using an integrated numerical model of the spaces and subsystem involved including the ground thermal response and the Trombe wall. The effectiveness of natural ventilation in achieving

thermal comfort is determined through the reliability of the proposed system in providing thermal comfort without having to rely on mechanical cooling during summer months for a case study in inland plateau in Lebanon characterized by dry hot climate.

CHAPTER 2

SYSTEM DESCRIPTION AND MATHEMATICAL FORMULATION

The proposed natural ventilation system is shown in Fig. 2.1 where outdoor air is first brought into the basement space where it exchanges heat with the cool basement walls, thus lowering its temperature. This cool air is driven upward into the living space under the buoyancy effect of a solar heated Trombe wall.

The effectiveness of the proposed air conditioning system relies on several factors: outdoor air temperature, solar heat flux and basement structure material and dimensions. Mathematical models for the Trombe wall, the space, ground, and the basement were developed, and then integrated for the purpose of predicting the indoor living zone air temperature and evaluating the system energy cost.

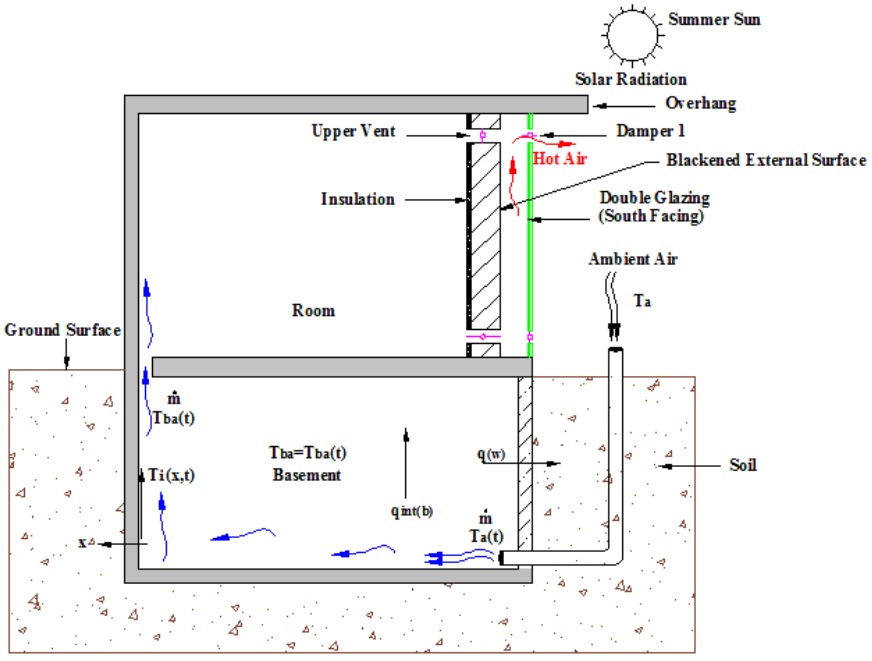

Fig. 2.1: Schematic diagram of the proposed system

2.1. Trombe Wall Model

The Trombe wall model is based on steady state one-dimensional energy balances performed on the glass cover, the air channel, and the absorber wall as presented by Ong and Chow (2003) in order to predict the air flow rate generated by the Trombe wall. To this end, the temperatures of the glass cover, the absorber wall, and the air in the flow channel are needed. Accordingly, the lumped system analysis for the glass surface temperature T_g, absorber wall T_w, and air temperature in the channel T_f was adopted, where the steady state energy balances for the glass cover, the air channel, and the absorber wall, shown in Fig. 2.2, were written as described in this section.

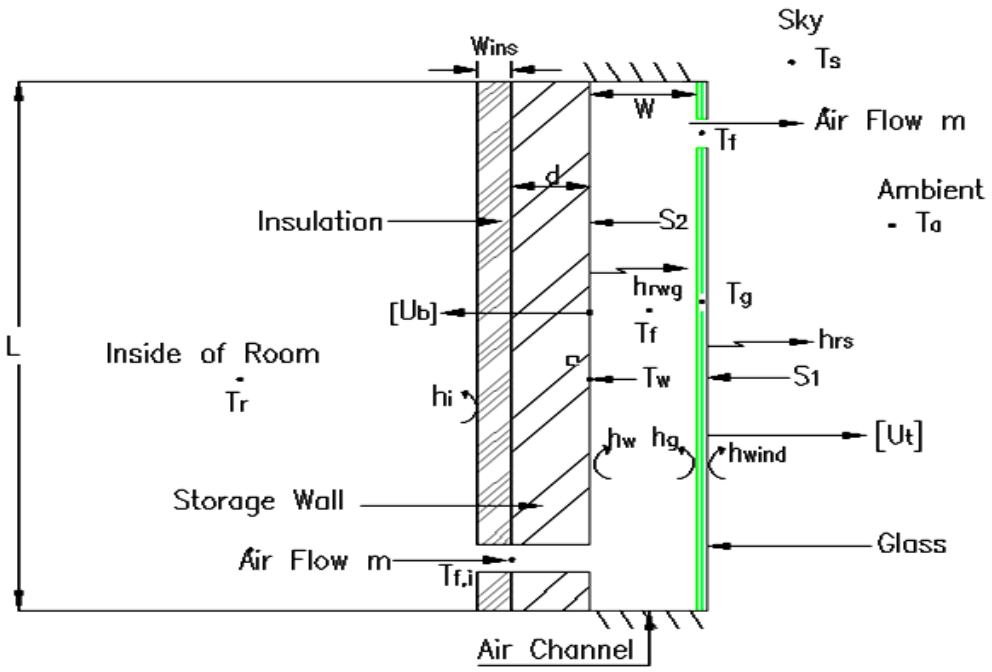

Fig. 2.2: Physical model of the Trombe wall

The glass cover exchanges heat with the air channel and the absorber wall and its energy balance is given by

$$\alpha_g I + h_{rwg}(T_w - T_g) + h_g(T_f - T_g) = U_t(T_g - T_a) \qquad (2.1.1)$$

where:

$$h_{rwg} = \sigma(T_g^2 + T_w^2)(T_g + T_w)/(1/\varepsilon_g + 1/\varepsilon_w - 1) \quad (2.1.2)$$

$$U_t = h_{wind} + h_{rs} \quad (2.1.3)$$

The convective wind heat loss coefficient, h_{wind}, and the radiative heat transfer coefficient between glass cover and sky, h_{rs}, were calculated as presented by Ong and Chow (2003). Whereas, the sky temperature (T_s) was estimated using the correlation given by Swinbank (1963). In Eq. (2.1.1), the first term represents the solar radiation heat flux absorbed by glass cover, the second term represents the radiative heat transfer between the vertical wall and the glass cover, the third term represents the convective heat transfer between the glass cover and the air channel, and the last term denotes the overall heat loss coefficient from top of the glass cover.

In the air channel, heat exchange between the glass and the absorber wall takes place as described by

$$h_w(T_w - T_f) = h_g(T_f - T_g) + \dot{m}c_f(T_f - T_{f,i})/WL \quad (2.1.4)$$

The air mass flow rate was determined using the buoyancy-driven stack effect equation presented by Allard et al. (1998) and is given by

$$\dot{m} = \rho_f C_d A\sqrt{\left(\frac{2\Delta T g H}{T_r}\right)} \quad (2.1.5)$$

where $\dot{m}$ is the air mass flow rate due to stack effect (kg/s); ρ_f is the density of air (kg/m^3); C_d is the opening's discharge coefficient (0.6 according to Flourentzou et al. (1998)); A is an opening's cross-sectional area (m^2) (assuming equal opening area for inlet and outlet); ΔT is the difference between indoor and air in channel temperature

(°C); g is gravitational acceleration; H is the distance between the midpoint of the inlet and the outlet (m); and T_r is room air temperature (°C).

Similarly, the absorber wall exchanges heat with the air channel and the glass and its energy balance is given by

$$\tau\alpha_w I = h_w(T_w - T_f) + h_{rwg}(T_w - T_g) + U_b(T_w - T_r) \quad (2.1.6)$$

where:

$$U_b = 1/(1/h_i + d/k_w + w_{ins}/k_{ins}) \quad (2.1.7)$$

In Eq. (2.1.6), the first term represents the solar radiation heat flux absorbed by the vertical wall, the second term denotes the convective heat transfer between the vertical wall and the air channel, the third term represents the radiative heat transfer between the vertical wall and the glass cover, and the last term denotes the overall conductive heat transfer between the vertical wall and the room.

2.2. Space Model

The objective of this model is to predict the temperature variations of the room air. This requires the following information: the space dimensions, characteristics of the construction materials, outdoor weather conditions, external and internal loads. Using the lumped approach while neglecting infiltration, the expression for the internal lumped air node energy balance is given by

$$\rho_f V_r c_f \frac{\partial T_r(t)}{\partial t} = \sum_{i=1}^{6} h_{cr} A_i (T_i - T_r) + \dot{m} c_f (T_{ba} - T_r) + \sum q_{\text{int}} \quad (2.2.1)$$

where: ρ_f, V_r, *and* c_f represent air density, room volume and air specific heat capacity respectively, A_i and T_i are the surface area and the temperature of the room

element $i, \dot{m}$ *and* T_{ba} are the mass flow rate and the temperature of the air supplied by the basement. q_{int} is the internal heat load.

However, the heat transfer by convection between room air and the space walls depends on the temperature of the walls. Accordingly, the transient one-dimensional heat conduction equation presented by Yassine et al. (2012) was adopted so as to determine the space wall temperatures. The heat transfer through the absorber wall is assumed one-dimensional while the storage effect is considered due to varying outdoor conditions and internal loads. Thus, the heat conduction across the absorber wall is given by

$$k_w \frac{\partial^2 T}{\partial x^2} - \rho_w c_w \frac{\partial T}{\partial t} = 0 \qquad (2.2.2)$$

The temperature of the outer (hot) surface of the wall determined by the Trombe wall model was used to study the heat flow across the absorber wall. Similar heat equations were developed for the upper space walls while imposing the appropriate boundary conditions (Yassine et al. 2012).

2.3. Basement Model

The basement space model aims to define the temperature variations of the basement air, T_{ba}, over time. A dynamic heat balance equation of the underground space presented by Kajtar et al. (2015) was adopted in this study. The heat balance of the underground space is given by

$$\rho_f V_b c_f \frac{\partial T_{ba}(t)}{\partial t} = q_{\text{int}(b)} - q_w(t) - q_s(t) \quad (2.3.1)$$

where $q_{int(b)}$ denotes the internal heat load in the basement including human, light, and electrical equipment components and $q_w(t)$ defines the convective heat transfer from the air to the wall and is given by

$$q_w(t) = \sum_{i=1}^{4} h_{cb} A_i (T_{ba}(t) - T_i(x,t)\big|_{x=0}) \quad (2.3.2)$$

where A_i and T_i are the surface area and the temperature of the room wall *i*. The heat performance of ventilation (supply air) is given by

$$q_s(t) = \dot{m} c_f \left[T_{ba}(t) - T_a(t)\right] \quad (2.3.3)$$

where $\dot{m}$ in *(kg/s)* and T_{ba} in *(°C)* are the mass flow rate and the temperature of the air supplied by the basement. T_a in (°C) is the ambient temperature.

In this study, ambient air is supplied to the basement through a soil buried tube at low level in order to prevent any air short-circuiting. Inside the basement, the ambient air exchanges heat with the basement cool surfaces. The moderated air is used then to condition the upper space as shown in Fig. 2.1.

The temperature of the heat sink is very important for determining the amount of heat that can be lost by the basement walls. Thus, the vertical temperatures distribution of the ground were modeled using the correlation provided by Labs and Cook (1989) who found that the temperature of the ground is a function of the time of year and the depth below the surface as follow:

$$T_{soil}(z,t) = T_{mean} - T_{amp} \times \exp(-z\sqrt{\frac{\pi}{365 \times \alpha}}) \times \cos(\frac{2\pi}{365}(t_{year} - t_{shift} - \frac{z}{2}\sqrt{\frac{365}{\pi \times \alpha}})) \quad (2.3.4)$$

where $T_{soil}(z,t)$ is the soil temperature at depth z (in m) on day t of the year; T_{mean} is the mean annual ground temperature (in °C); T_{amp} is the annual temperature amplitude at the surface ($z=0$, in °C); z is the depth (in m); t_{year} is the time of the year (in days); t_{shift} is the phase constant, the day of minimum surface temperatures; α is the thermal diffusivity of the soil (in m^2 per day).

Eq. (2.3.4) was used to determine the temperature of the soil underneath the basement's floor, while an average temperature must be used for the earth-contact wall profile since the wall realistically extends for several meters in the soil, where the temperature changes with depth. Therefore, the average temperature of any specified wall profile, ranging from the top of the wall at depth a to the bottom of the wall at depth b, can be determined by integrating Eq. (2.3.4) with respect to depth and dividing by the height of the profile $(b-a)$. Accordingly, Eq. (2.3.4) can then be expressed as presented by Al-Temeemi and Harris (2003)

$$T_{soil}(a-b,t) = T_{mean} + \frac{T_{amp}}{\sqrt{2(\pi/365\alpha)}(a-b)} \times \exp(-z\sqrt{\frac{\pi}{365\times\alpha}}) \times \cos(\frac{2\pi}{365}(t_{year} - t_{shift} - z\sqrt{\frac{\pi}{365\times\alpha}}))\Big|_b^a \quad (2.3.5)$$

The values from Eq. (2.3.5) were used for the outer boundary temperature conditions for the simulation of the below grade wall section using the same transient one-dimensional heat conduction equation that was adopted for the absorber wall. The basement model assumes that the temperature of the soil changes in accordance with the change of season. This change means that a certain delay and damping in soil temperature takes place as depth of soil increases. The amplitude of the temperature change is 0.6 °C in the depth of 8 m and 0.2 °C in the depth of 10 m (Kajtar et al. 2015). The location of the underground space under the earth's surface determines the sizing soil temperature. Further, the heat capacity of the soil is considerably higher than that of

the air. Thus, according to these aspects, the soil temperature can be considered to be quasi-stationary. Moreover and due to the high thermal inertia of the soil, the temperature fluctuations at the surface of the ground are decreased as the depth of the ground increments. Accordingly, daily ground temperatures were considered rather than hourly ones (Florides and Kalogirou 2004). The soil is assumed a homogeneous material in terms of heat transfer properties with its resultant thermal characteristics (Kajtar et al. 2015).

The humidity load of the underground space was negligible, thus the air exchange happens at constant absolute humidity. For this situation, the absolute humidity content can be viewed as equivalent to the absolute humidity content of the supply air. The concrete walls were considered to have similar thermal characteristics as the soil (Kajtar et al. 2015).

2.4. Thermal Comfort Model

Several studies introduced different thermal comfort models (ASHRAE standard 55 1992; Fanger 1970; Kruger 2008; Zhang et al. 2010). Moreover, ASHRAE standard 55 (2001) addressed a new adaptive comfort model for buildings that rely on natural ventilation. To this end, this standard was adopted in this study since no mechanical system is being used.

The outdoor climatic environment is characterized in terms of mean outdoor dry bulb temperature $T_{a,out}$. The optimum comfort temperature, T_{comf}, is then calculated based on mean $T_{a,out}$ and is given by

$$T_{comf} = 0.31 \times T_{a,out} + 17.8 \qquad (2.4.1)$$

where $T_{a,out}$ and T_{comf} are expressed in °C.

The next step was to define a range of temperatures around T_{comf} corresponding with 80% thermal acceptability as per the new adaptive comfort standard for ASHRAE standard 55 (2001).

CHAPTER 3

NUMERICAL SIMULATION METHODOLOGY

This study used numerical finite difference method in order to predict the performance of the integrated system shown in Fig. 2.1. All the equations and the subsystem models that were presented earlier are coupled together using an implicit first-order time integration scheme and second order spatial discretization for the wall nodes so as to get the full model that evaluates the effectiveness of the proposed system. This was achieved by presenting the mathematical models for each of the Trombe wall, the space, the adjacent ground, and the basement model and integrating these models into one model that included all the physical parameter and schedules of the integrated zone. Input data for geometry, boundary and initial conditions were compiled for the following models: the Trombe wall parameters, the space and the basement dimensions, the construction materials characteristics, external and internal loads, and the outside climate conditions. The integrated model is capable of determining the amount of ventilation air that can conceivably give indoor thermal comfort for longer periods and hence minimize the number of discomfort hours.

Equation (2.2.2) was solved numerically using fully implicit finite-difference form. The considered scheme is first order in time and second order in space where each wall layer was decomposed into a number of control volumes. The total number of nodes used was 70 nodes. The integrated model was developed using MATLAB© and then simulated to obtain the indoor zone thermal comfort when subjected to variable external and internal loads as indicated in the flow chart (see Fig. 3.1).

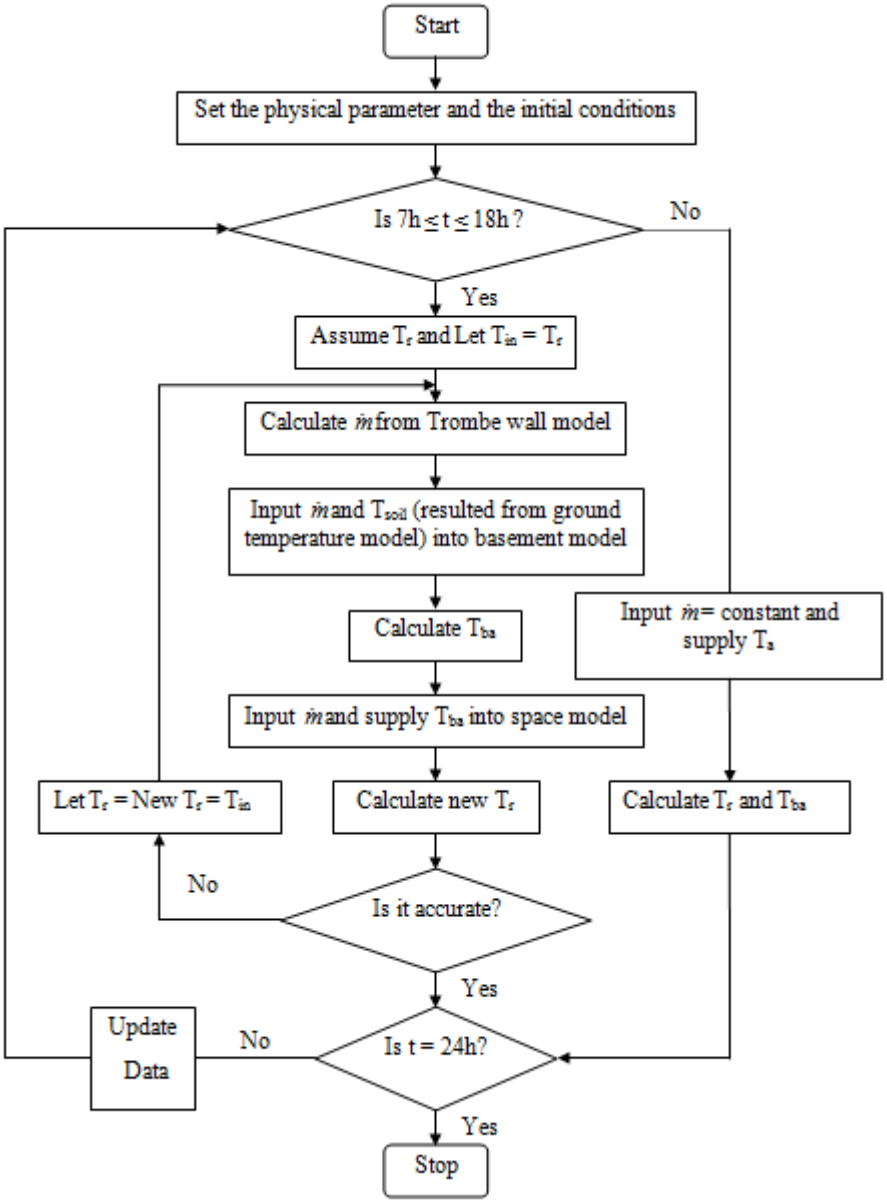

Fig. 3.1: Numerical model flow chart

Starting from the temperature of the outer (hot) surface of the absorber wall determined by the Trombe wall model as a boundary condition, and using a time step of 360 s, the inner surface temperatures of the absorber wall as well as the space walls were computed. Simulations are performed for a typical summer day of each month (June through September) to obtain the effectiveness of the proposed system in

providing thermal comfort throughout the entire day. At the end of the 24 h operational period of each month, the initial conditions were recalculated and used as input in the cyclic simulations until steady periodic convergence was achieved. The criterion for convergence is reached when the maximum percentage error for air temperature between the simulation values at time t and t + 24 h is less than 10^{-4}%.

The flow chart shown in Fig. 3.1 summarizes the path followed to calculate the needed output from the developed model.

CHAPTER 4

VALIDATION OF THE TROMBE WALL MODEL

The developed Trombe wall mathematical model was validated against published experimental results (Kongduang 1997). In the description of Kongduang' experiment, a small model of a solar house with 2.68 m height and base area of 3.35 × 3.45 m was built. It had one window and one door with an air grille on the north side. A metallic solar wall (MSW) was integrated to the south wall of the house. The other three sides of the house were made of plywood and gypsum plate. The roof was made of CPAC Monier concrete tiles (33 cm × 42 cm × 1.5 cm) in a dark red color. The floor was made of plywood supported by concrete beams. The MSW was 1 m wide and 2 m high. It consisted of zinc plate, micro-fiber and plywood with thickness of 0.7, 25, and 4 mm respectively. Its outer surface was painted matt black and covered with commercial glass of 5 mm thickness. A pair of centered vents, 25 cm × 5 cm each was located at the bottom of the metallic plate (room side) and another pair near the top of the cover. There was an air gap between the wall and the cover. The reported design of MSW allowed varying the height (1-2 m) and air gap (10-14.5 cm). A set of type-K thermocouples were used to measure the temperature at several points of the MSW and at six points inside the room elevated 1 m from the floor. Measurements were taken for different gaps (10-14.5 cm), different heights (1-2 m), and different mean solar intensities (385, 406, 422, and 535 W/m^2).

The experimental investigations of the performance of the MSW showed that with 2 m height and 14.5 cm gap, the MSW would produce optimum natural ventilation. Accordingly, the developed Trombe wall mathematical model was validated against the

experimental data of the MSW presented by Kongduang (1997) under similar optimum setups.

Several inputs were used in order to run the developed Trombe wall model such as: the hourly variations of the ambient air temperature on the day of the experiment (see Fig. 4.1(a)), the hourly profile of the solar radiation, the physical and thermal properties of the MSW and the glass cover, properties of the air, the dimensions of the vents, and the air gap between the wall and the glass cover. Relevant parameters used for the calculations are summarized in Table 4.1. Note that the room temperature profile was given and It was similar to the profile of the ambient temperature on the day of the experiment. Also, the hourly profile of the solar radiation in Bangkok was generated so as to end up with the same given mean on the day of the experiment. Moreover, the inlet temperature of air in the channel was assumed to take place at room temperature. The developed Trombe wall generates the hourly temperature variations of each component of the MSW (cover, air and metallic plate) as an output. In addition, it gives the hourly variations of the air mass flow rate produced by the MSW.

Fig. 4.1(a) shows a comparison between simulated and measured temperatures of metallic plate, T_m, and air gap, T_f. The two profiles were relatively identical except in the afternoon where the metallic plate temperatures were slightly underestimated and the temperatures in the air gap were overestimated a little bit. Fig. 4.1(b) shows a comparison between simulated and experimental air mass flow rate produced by the MSW. The difference between the simulated and published measured results of Kongduang (1997) was about 9%. The good agreement with measured published results validated the current developed Trombe wall model.

Table 4.1: Metallic solar wall (MSW) parameters (Kongduang 1997)

Parameter	**Value**
Absorptance-transmittance product ($\tau\alpha$)	0.682
Plywood thermal conductivity, k_w (W/m·K)	0.138
Micro-fiber thermal conductivity, k_{in} (W/m·K)	0.0324
Zinc thermal conductivity, k_m (W/m·K)	112.2
Plywood surface emissivity, ε_w	0.9
Metallic surface emissivity, ε_m	0.6
Glass surface emissivity, ε_C	0.94
Discharge coefficient, C_d	0.8
Air gap (cm)	14.5
MSW height (m)	2
Zinc plate thickness (mm)	7
Micro-fiber thickness (mm)	25
Plywood thickness (mm)	4

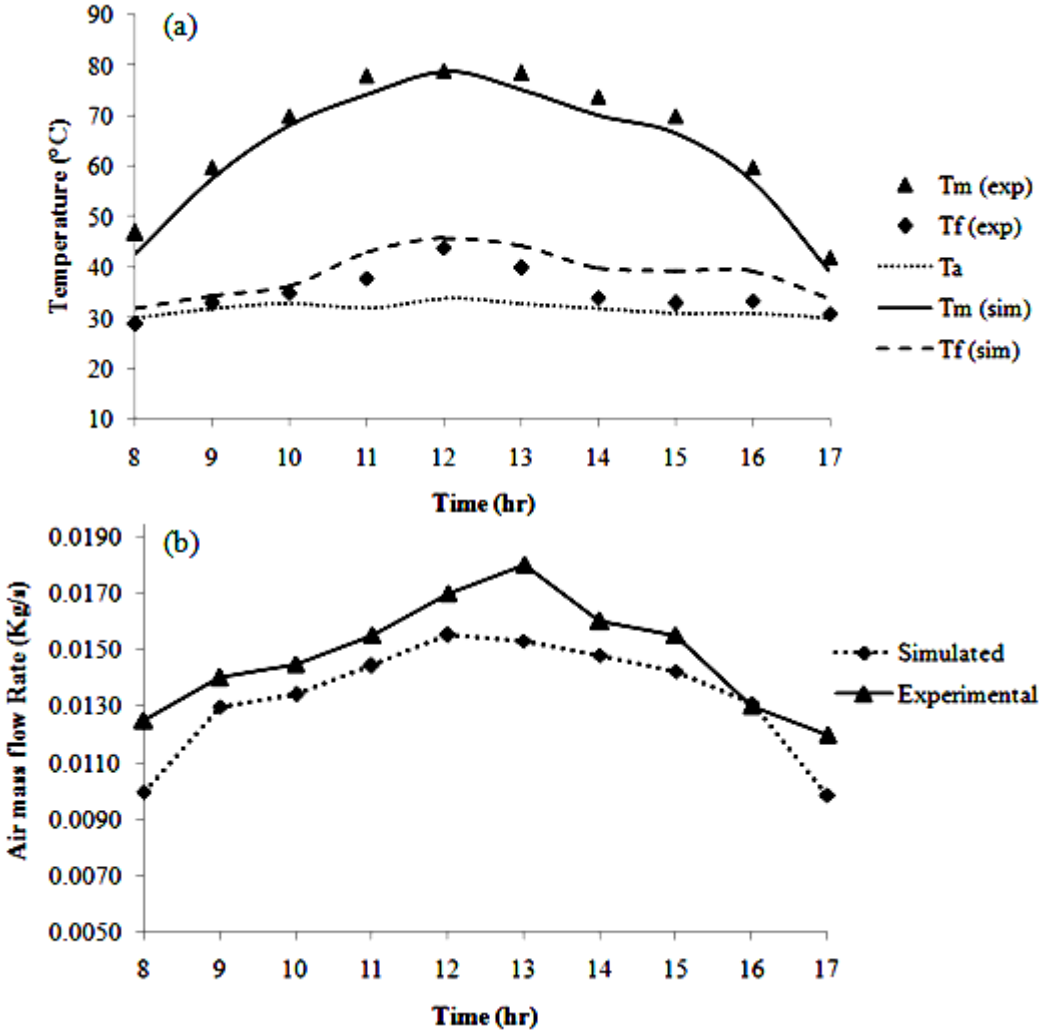

Fig. 4.1: (a) Comparison between simulated and measured temperatures of metallic plate and air gap and (b) Comparison between simulated and experimental air mass flow rate produced by the MSW with 14.5 cm air gap and 2 m height (Kongduang 1997)

CHAPTER 5

CASE STUDY

A small isolated single living room unit with a basement was considered as a base case in the assessment of the performance of the proposed natural ventilation system described prior in this study (see Figs. 5.1(a) and 5.1(b)). This unit was assumed located in the inland district (zone 3) of Lebanon. It had a rectangular shape with a base area of 6 m × 5 m and a ceiling of 2.8 m height. It is exposed to the outside from two sides. The external walls are made of 15 cm hollow blocks with 1 cm of mortar cement plaster on the interior and exterior side of the wall. The roof is insulated and built of 20 cm reinforced concrete with 1 cm of mortar cement plaster on the interior side. This is typical Lebanese building materials. The external walls had an overall heat transfer coefficient of 2.36 $W/m^2 \cdot K$ and a heat capacity of 1200 J/kg while the roof had an overall heat transfer coefficient of 1.67 $W/m^2 \cdot K$, which is typical for urban residential apartments in Lebanon (Republic of Lebanon Ministry of Public Works and Transport 2005). A basement space of an area of 6 m × 5 m was located underneath the living room unit and immersed to a depth of 2.5 m in a sandy clay loam soil that had the following thermal characteristics: thermal diffusivity of 0.316×10^{-6} m^2/s, thermal conductivity of 0.503 W/m·K, and heat capacity of 1.59×10^3 $kJ/ m^3 \cdot K$. The basement walls were all made of 20 cm reinforced concrete with 3 cm cement plastering as an interior finishing, whereas the basement floor was made of concrete tiles.

The internal load component was based on the occupancy schedule of a typical Lebanese family consisting of six persons (Republic of Lebanon Ministry of Public Works and Transport 2005). Figs. 5.2(a) and 5.2(b) demonstrate the schedule of

occupancy and the schedule of the electrical load in the living zone during the sunshine hours respectively. The electrical loads were 10 W/m^2 of sensible load for lighting fixtures and 800 W for appliances. This schedule was considered for the summer time. The weather data (outdoor air temperature, solar radiation, wind speed and relative humidity) was obtained from the Advancing Research, Enabling Communities (AREC) that was used by Fawaz et al. (2013).

Trombe wall is integrated into the south wall of the living space as shown in Fig. 5.1(b). A masonry wall of 0.4 m thickness, coated with a dark, heat absorbing material and covered by a double layer of glass, placed from about 0.3 m away from the masonry wall was selected. The detailed parameters of Trombe wall are listed in Table 5.1.

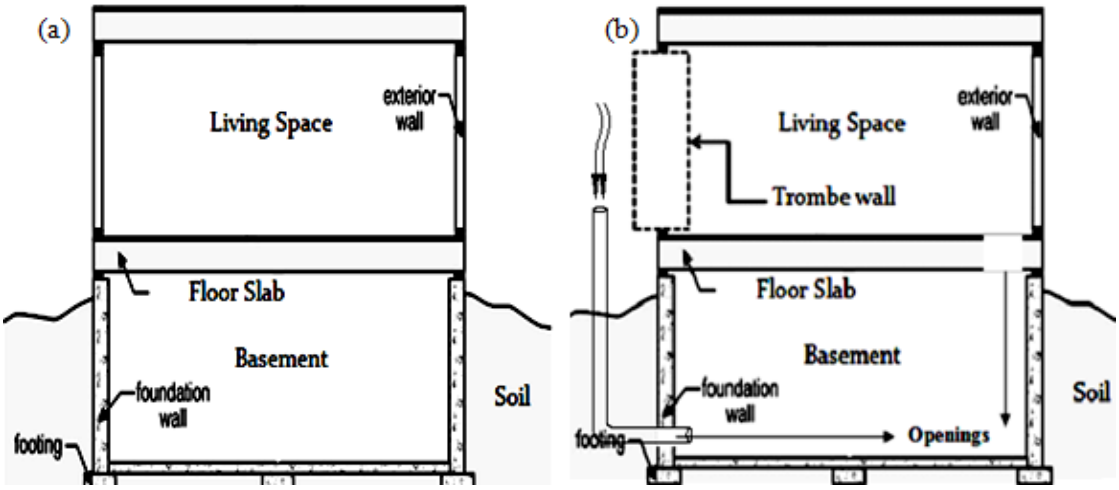

Fig. 5.1: Cross section of an isolated living space with a basement (a) for a typical construction and (b) when integrated with Trombe wall

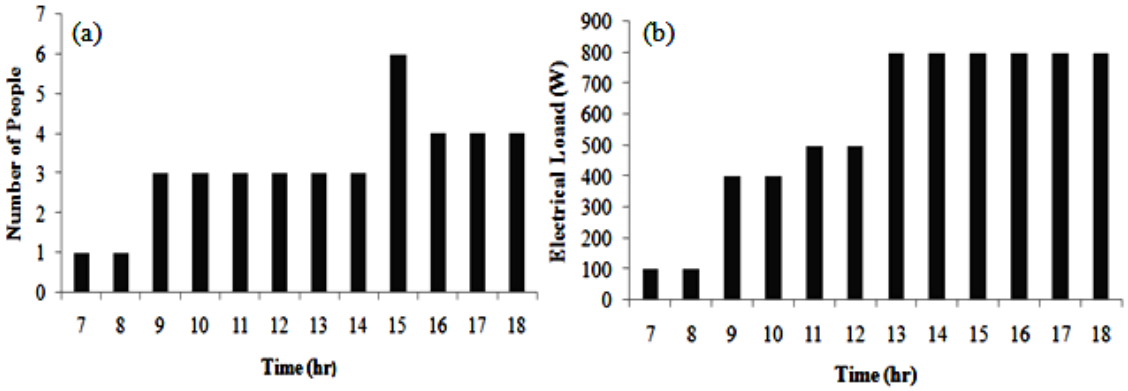

Fig. 6.2: (a) Schedule of occupancy and (b) Schedule of electrical loads inside the living space during sunshine hours

Table 5.1: South-oriented Trombe wall parameters

Parameter	Value
Absorptance-transmittance product ($\tau\alpha$)	0.728
Wall thermal conductivity, k_w (W/m·K)	1.8
Insulation thermal conductivity, k_{in} (W/m·K)	0.032
Wall emissivity, ε_w	0.2
Glass surface emissivity, ε_g	0.75
Discharge coefficient, C_d	0.6
Air gap (cm)	30
MSW height (m)	2.8
Wall thickness (mm)	400
Insulation thickness (mm)	50

The developed model includes all the physical parameters and schedules of the integrated zone and it provides the cooling requirements for the space that define the

required values of the system variables to achieve thermal comfort. The objective of this study is to show the benefits of the integrated system in reducing the cooling energy needs and enhancing thermal comfort.

5.1. Comfort and System Performance of the Case Study

The main purpose of utilization the Trombe wall in this study was that it generates the buoyancy needed to draw the cooler air from the basement as mentioned earlier. But to do so, Trombe wall needs sufficient solar energy in order to heat the absorber wall that drives the stack effect without increasing the room temperature. This was the case during the sunlit hours. However, during night when solar energy is not sufficient to activate the Trombe wall and to drive the basement air, a mechanical fan operating at the minimum outdoor air requirements of 15 cfm (7.5 L/s) per person for ventilation of residential facilities as per ASHRAE standard 62.1 (2004) was utilized in order to moderate the temperature of the space and to prevent overheating.

Simulations were performed for the case study described in the above section on a representative summer day, i.e. the 15^{th} of each month (June through September) for the Bekaa region that is situated in East of Lebanon in order to examine the effectiveness of the proposed system in providing thermal comfort throughout the summer time. In order to obtain accurate results independent of the initial conditions assumed for the room air and wall temperatures, simulations were performed for 3 consecutive days, and the data for the third day were adopted in the analysis.

In Fig. 5.3(a), the relationship between the ambient temperature, the indoor room temperature, and the basement temperature during the month of June is given while the resulting air mass flow rate for this month is shown in Fig. 5.3(b). In the same

manner, the relation between temperatures and the induced air mass flow rate for the months of July, August, and September are shown in Figs. 5.4(a), 5.4(b), 5.5(a), 5.5(b), 5.6(a), and 5.6(b) respectively.

For the month of June and during the natural cooling mode, Trombe wall was operational for the sunshine hour extending from 7 h to 18 h and it was very clear from Fig. 5.3(b) that the induced air flow rate increased with increasing solar radiation, that definitely expanded wall heat gain, and it was noticed that the airflow rate varies from 0.0407 Kg/s to maximum of 0.0972 Kg/s during this month. Moreover, it was found that the lowest value of the ventilation air was occurred during this month at 18 h where the solar intensity was relatively very low (324 W/m^2), and it was close to 0.0407 Kg/s. However, during the forced airflow mode, external air was drawn into the living space using a constant speed fan that was turned on continuously at a constant air flow rate of 0.04 Kg/s. This can provide sufficient rates of air movement in the living space (about 1.4 ACH) which complies with the minimum outdoor air requirements for ventilation of residential facilities recommended by ASHRAE standard 62.1 (2004) (see Fig. 5.3(b)). Note that during the forced airflow mode, the basement was treated as a closed system thus, no air flow was coming into it or getting out of it.

For the remaining summer months (July through September), similar air flow rates trend was noticed (refer to Figs. 5.4(b), 5.5(b), and 5.6(b)) providing that the peak value of the ventilation air was occurred in August at 12 h during the daytime when high solar intensity was strong enough (1258 W/m^2), and it was close to 0.1023 Kg/s.

The comparison of ambient, basement and room air temperature during the month of June is shown in Fig. 5.3(a). It can be seen from this figure that under the natural airflow condition, the supply basement air temperature was almost in the range

of 19-26.9 °C where the outdoor air temperature was following the shown temperature profile (refer to Fig. 5.3(a)). The difference between the ambient and basement temperature was in the range of 1.3-7.2 °C. Furthermore, It was noticed that the room air temperature fluctuated in a range of 22.7-30.1 °C. Accordingly, and based on the acceptable operative indoor temperature ranges that were determined for each month as recommended by the new adaptive comfort standard for ASHRAE Standard 55 (2001) (see Table 5.2), only 2 discomfort hours (occurred between 13 h and 15 h) were resulted during this month. Note that the mean outdoor air temperature was evaluated for the whole month and not for the typical day considered in order to determine the acceptable operative indoor temperature ranges. It worth pointing out that the main reason behind the noticed discomfort hours is that the supply basement air temperatures were not cool enough to moderate the indoor air temperatures as a result of the high ambient temperatures during these hours. On the other hand, during the night and until the sunrise, the assisted mechanical fan was turned on at the constant air flow recommended by ASHRAE standard (2004) and it was bringing outside air directly to the living space unlike the Trombe wall that was bringing basement air into the space. Thus, the pattern of the supply air temperature changed after the forced airflow mode was initiated for the period hour extending from 19 h to 6 h with the supply ambient air was in the range of 12.1-31.2 °C (see Fig. 5.3(a)). Besides, It was noticed from the profiles of the basement and the ambient air temperature that there was a big gap between the two profiles during the sunshine hours when the basement was treated as an open system and this is mainly due to the much greater (approximately 1325 times) heat capacity of the sandy clay loam soil as compared to air (1.59 vs. 0.0012 MJ/ m^3·K). However, this gap became

smaller during the night when the ambient air temperature was gradually dropped (refer to Fig. 5.3(a)).

Similar behavior was observed for the rest of the months (July through September) as shown in Figs. 5.4(a), 5.5(a) and 5.6(a) where 3 discomfort hours (occurred between 11 h and 14 h) were resulted during July as compared to 5 discomfort hours (occurred between 11 h and 16 h) during August, and 4 discomfort hours (occurred between 11 h and 15 h) during September.

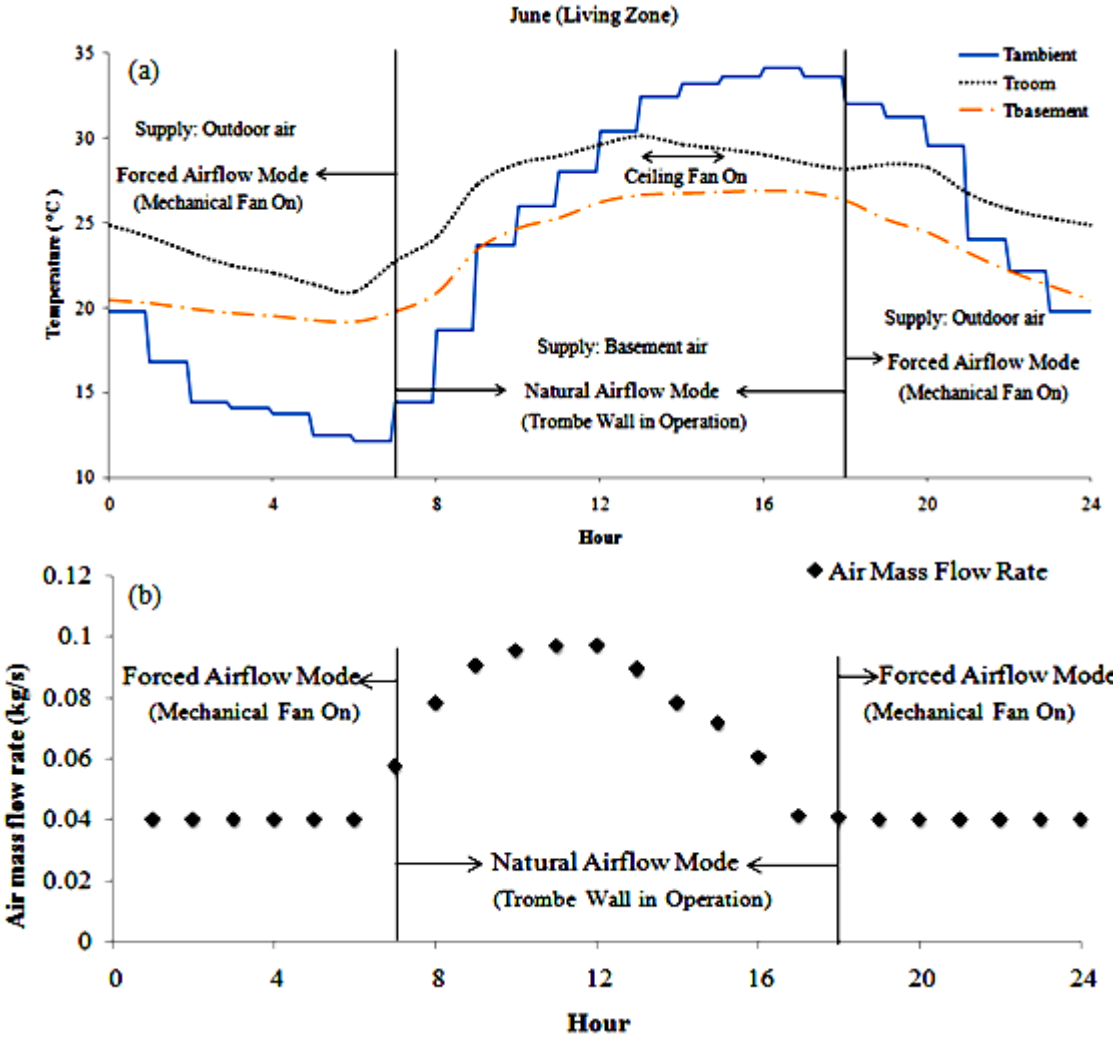

Fig. 7.3: (a) Predicted temperatures and (b) induced air mass flow rate in the living zone during June

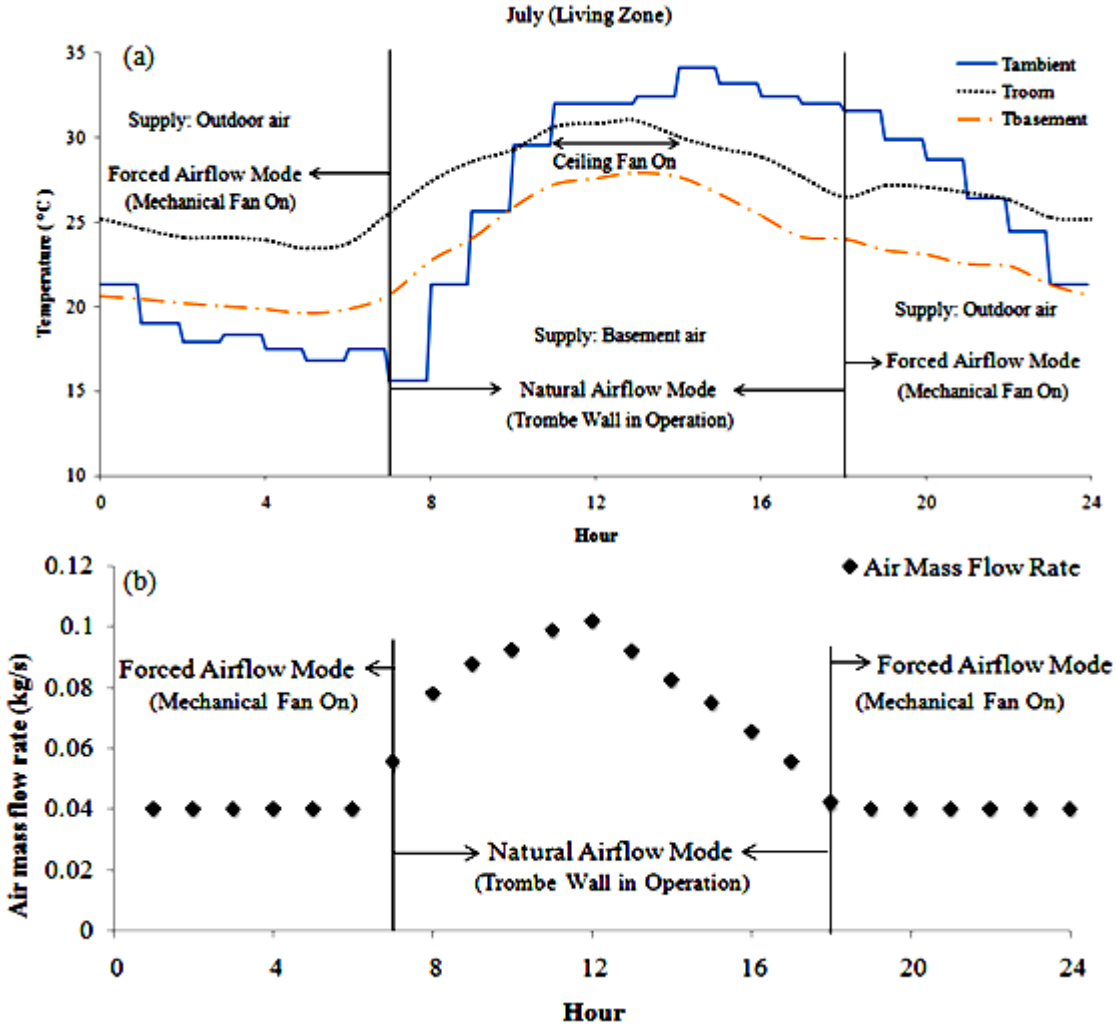

Fig. 8.4: (a) Predicted temperatures and (b) induced air mass flow rate in the living zone during July

Proceeding from the above results, the number of discomfort hours occurred during each month were multiplied by the number of days in each month to determine the monthly number of discomfort hours in the living space as shown in Fig. 5.7. Thus, for the sunshine hour period extending from 7 h to 18 h (natural airflow mode), the 80% acceptable thermal comfort condition can be provided for about 83.3% during month of June, 75% during July, 58.3% during August, and 66.7% during September. To further enhance thermal comfort inside the space and to reduce the discomfort hours to zero,

the ceiling fan was activated when the temperature inside the space increases beyond the maximum acceptable operative indoor temperature for each month as described in Table 5.2 (see Figs. 5.3(a), 5.4(a), 5.5(a) and 5.6(a)).

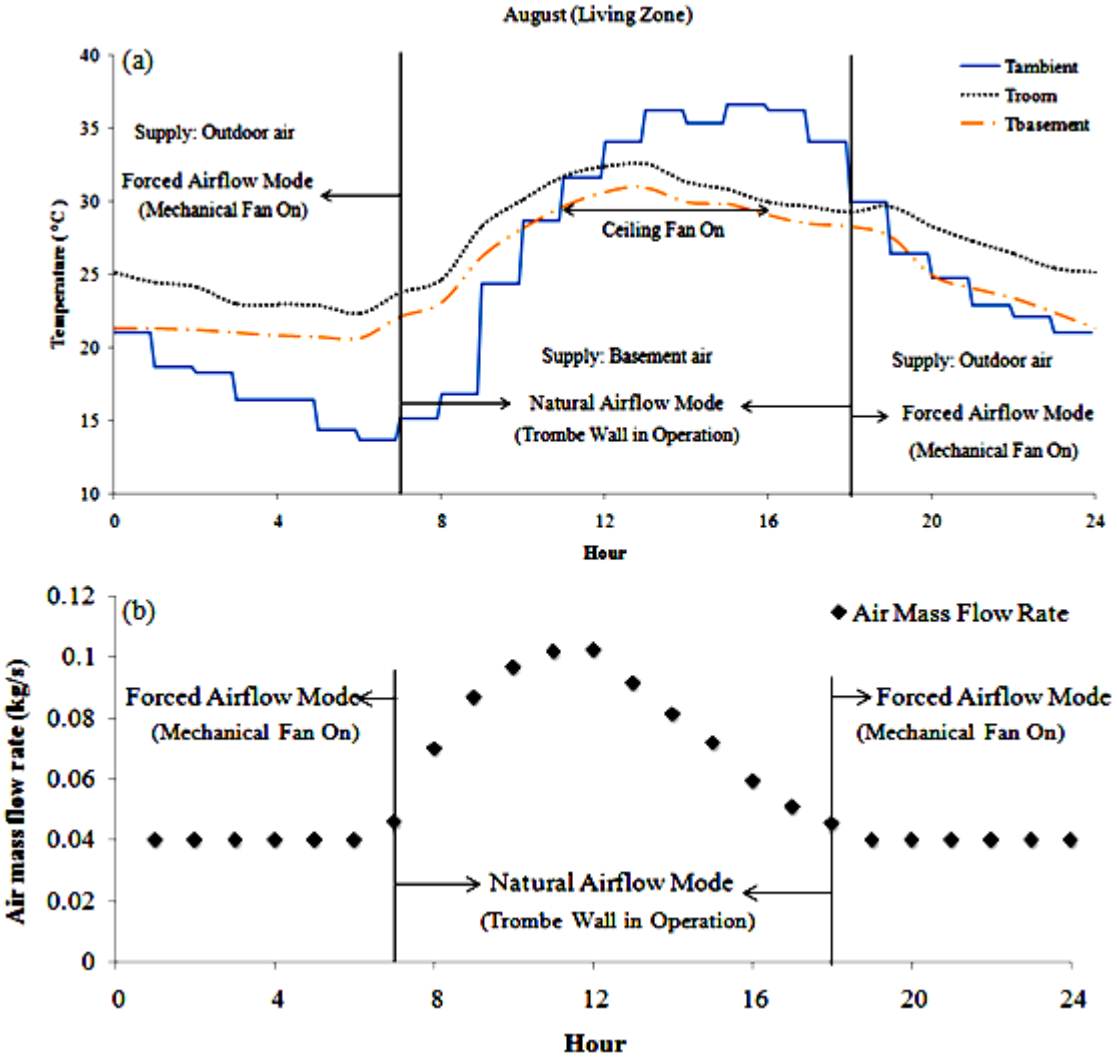

Fig. 9.5: (a) Predicted temperatures and (b) induced air mass flow rate in the living zone during August

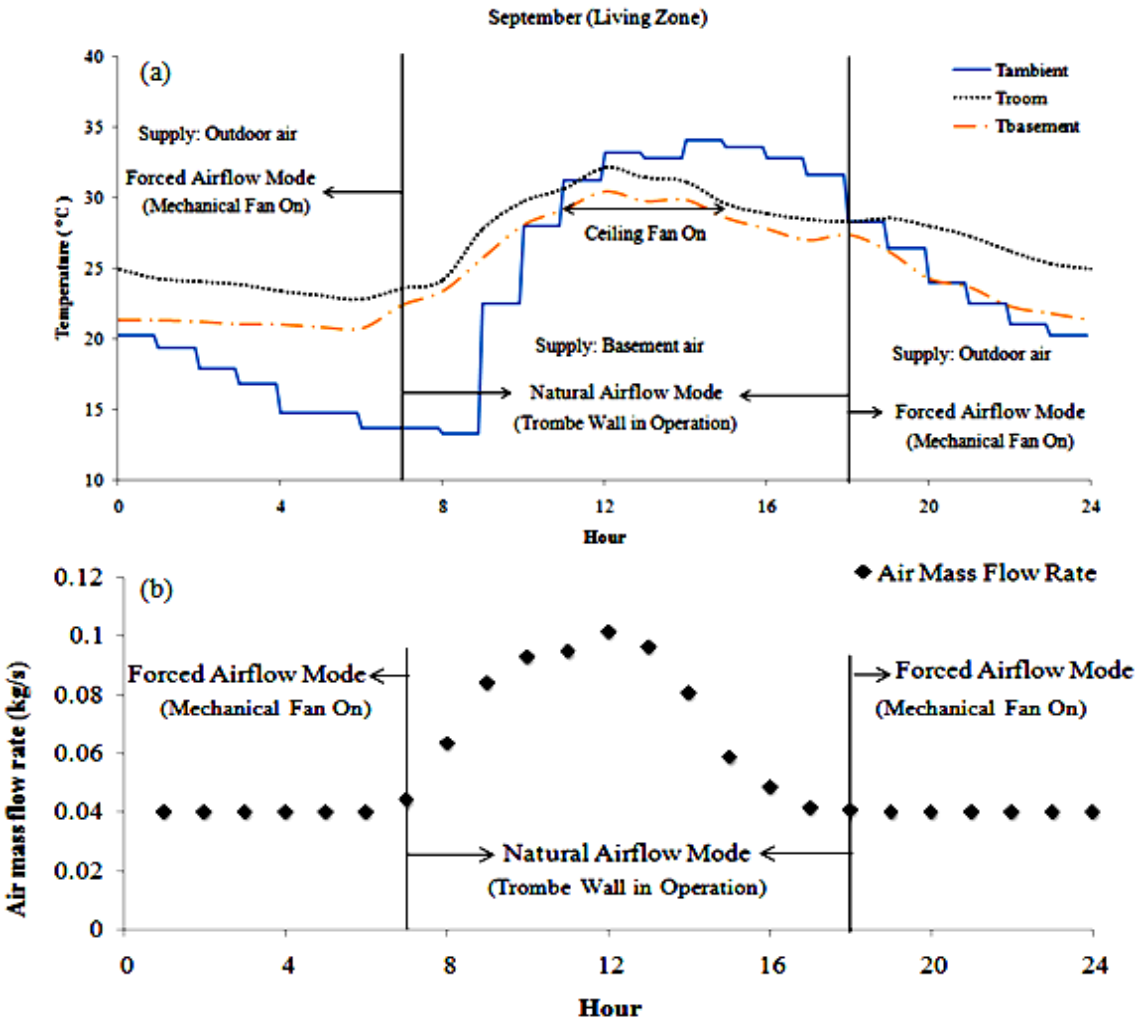

Fig. 10.6: (a) Predicted temperatures and (b) induced air mass flow rate in the living zone during September

Table 5.2: Required indoor operative temperature limits for naturally ventilated spaces in Lebanon (zone 3) as per the new adaptive ASHRAE standard 55 (2001)

Month		**June**	**July**	**August**	**September**
Mean Monthly Outdoor Air Temperature (°C)		27.7	30.1	29.8	27.3
80% Acceptability	**MIN**	22.8	23.5	23.4	22.7
	MAX	29.8	30.5	30.4	29.7

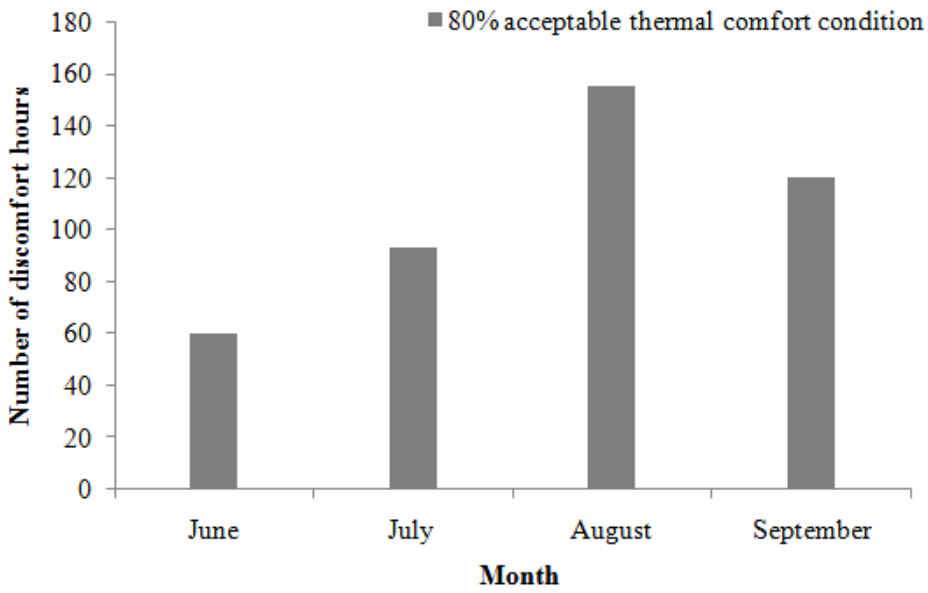

Fig. 11.7: Number of discomfort hours for 80% acceptable thermal comfort condition in the living zone during the sunshine hours (June through September)

Moreover, these results were benchmarked with a similar study conducted by Yassine et al. (2014) where an earth to air heat exchanger (EAHE) was used as a cooling source and it was noticed that the two systems had almost the same potential in providing indoor thermal comfort for the whole occupied period in the living zone.

In conclusion, the results showed that the proposed system in this study was capable of coping with internal heat gains of the typical residential house in Lebanon. It reduces the cooling energy demand. The savings in electrical power were calculated in terms of the energy needed for using a mechanical fan to maintain the same thermal comfort level attained by the proposed passive system during the natural airflow period, providing that the mechanical fan will be bringing more outside air than the basement air brought by the Trombe wall to result in the same room air temperature. The needed fan power was calculated based on the affinity law. Note that the ceiling fan power was not considered as it kept as an option to further enhance thermal comfort. Fig. 5.8

demonstrates the energy savings attained in the living zone when adopting the proposed system. The highest energy saving was reached during the month of August with 36.43 kWh while it reached its lowest value during the month of September with 14.92 kWh. In June and July, the energy savings were found to be 27.5 and 31.47 kWh respectively.

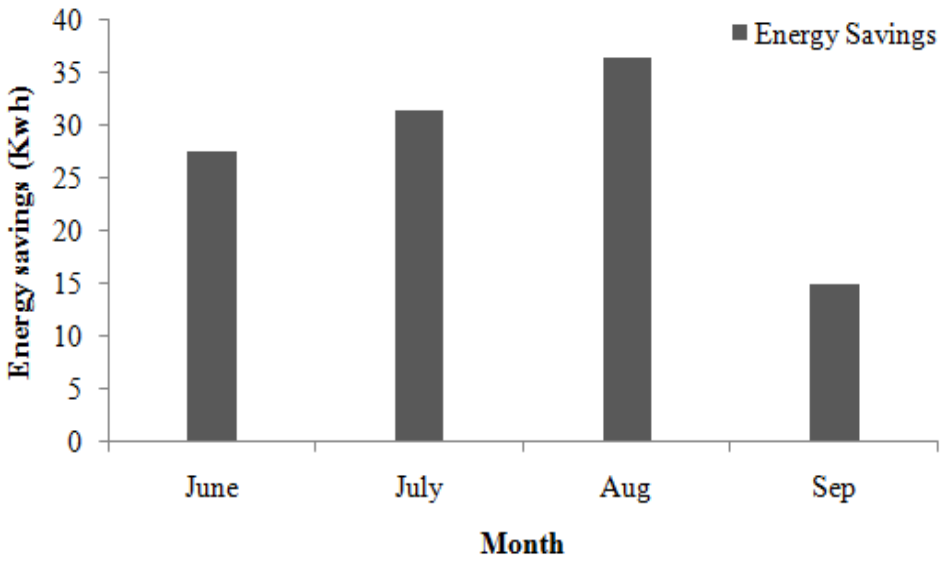

Fig. 12.8: Energy savings in the living zone during the sunshine hours (June through September)

5.2. Economic Analysis of the Proposed System vs. a Mechanical Ventilation System

In order to estimate the economic feasibility and efficiency of the proposed system, it was compared to a mechanical ventilation system, as mentioned earlier, that can attain the same indoor conditions as that of the proposed system with the condition that mechanical ventilation rates should be increased to match the indoor comfort level resulting from the Trombe wall driving the cooler air. If a mechanical ventilation system

is to be considered, the total electric energy consumption of the ventilation fan over a period of 4 months (June through September) was estimated to be 110.32 kWh. The cost of electricity in the inland district (zone 3) of Lebanon is estimated as 0.13 $/kWh. Therefore, the cost of electricity consumption by the mechanical ventilation system over the operational period of 4 months per year is calculated to be $14.3. As for the proposed system, the incremental cost of adding glazing cover window in front of the wall with the required vents and dampers was considered. Ultimately, the average completed Trombe wall costs $119. Hence, the payback period is about 8 years.

CHAPTER 6

CONCLUSION

This paper integrates Trombe wall, space, and basement models into one model. It was shown that using the proposed system was possible as a means of natural ventilation of a house with a basement, but there should be through study in the details of the house as well as its surrounding area so that the proposed system can work at its highest efficiency.

Through simulation, the integrated model showed that it can reduce significantly heat gain in the house by developing air circulation to provide indoor thermal comfort for longer periods thus, reducing the discomfort hours. The proposed system showed that it is promising in saving energy while attaining the thermal comfort needed and it was economical due to little cost of materials used. Also, the passive use of solar energy is energy efficient. The described passive system presented here could also be used with reverse function, i.e. to admit ambient air and to inject hot air into the house in cooler regions to provide heating during winter.

REFERENCES

Allard, F., Santamouris, M., Alvarez, S., European Commission., & ALTENER Programme. (1998). "Natural ventilation in buildings: A design handbook." London: James & James (Science Publishers) Ltd.

AI-Motawakel, M., Norton, B., Probert, S. (1987). "Solar energy harnessing performance of direct gain and non-vented Trombe walls under Yemeni weather conditions." Appl. Energy 26, 159-191.

Al-Temeemi, A. A., Harris D. J. (2003). "The effect of earth-contact on heat transfer through a wall in Kuwait." Energy Build 2003;35:399e404. Available from: www.sciencedirect.com [Accessed 1.03.2015].

ASHRAE, Climate, Comfort, and Natural Ventilation (2001). "A New Adaptive Comfort Standard for ASHRAE Standard 55." University of California, Berkeley.

ASHRAE. ASHRAE Standard 55 (1992). "Thermal Environmental Conditions for Human Occupancy." ASHRAE, Atlanta.

ASHRAE. ASHRAE Standard 62.1 (2004). "Ventilation for Acceptable Indoor Air Quality." Atlanta, GA: American Society of Heating, Refrigerating and Air-Conditioning Engineers, Inc.

Badescu, V., Isvoranu, D. (2011). "Pneumatic and thermal design procedure and analysis of earth-to-air heat exchangers of registry type." Applied Energy 88 (4) 1266–1280.

Energy efficiency and renewable energy (EERE) website (2009). U.S. department of energy.

Fanger, P. O. (1970). "Thermal Comfort." Danish Technical Press, Copenhagen.

Fawaz, H., Abiad, M., Ghaddar, N., Ghali, K. (2014). "Solar-assisted localized ventilation system for poultry brooding." Energy and Buildings, Volume 71, Pages 142-154.

Florides, G., Kalogirou, S. (2004). "Measurements of Ground Temperature at Various Depths." Proceedings of the SET 2004, 3rd International Conference on Sustainable Energy Technologies on CD-ROM, Nottingham, UK.

Flourentzou, F., Van der Maas, J., Roulet C. (1998). "A natural ventilation for passive cooling: measurement of discharge coefficients." Energy and Buildings 27:283–92.

Ford, B. (2002). "The Architecture of Cooling Without Air Conditioning." SAMSA 2002 Lecture Material.

Froland-Larson, A. (2001): Energieverbrauch für Lüftung, in: DANVAK Fachzeitschrift Nr. 2: Jnr 598F502A.

Gan, G. (1998). "A parametric study of Trombe walls for passive cooling of buildings." Energy Build. 27, 37–43.

Ghrab-Morcos, N., Bouden, C., Franchisseur, R. (1993). "Overheating caused by passive solar elements in Tunis. Effectiveness of some way to prevent it." Renew. Energy 3 (6/7), 801– 811.

Grosso, M., Raimondo, L. (2008). "Horizontal air to-earth heat exchangers in Northern Italy – Testing, design and monitoring." International Journal of Ventilation 7 (1) 1–10.

Ibn-Mohammed, T., Greenough, R., Taylor, S., Ozawa-Meida, L., Acquaye, A. (2013). "Operational vs. embodied emissions in buildings - a review of current trends." Energy Build 66:232-45.

IEA (2013). "Transition to sustainable buildings: strategies and opportunities to 2050." International Energy Agency (IEA).

IEA (2013). "World Energy Outlook 2013." International Energy Agency (IEA).

Kajtar, L., Nyers, J., Szabo, J. (2015). "Dynamic thermal dimensioning of underground spaces." Energy, 87: 361-368.

Kleiven, T. (2003). "Natural ventilation in buildings: architectural concepts, consequences and possibilities." Norwegian University of Science and Technology.

Kongduang, W. (1997). "Study of the natural ventilation of houses by a metallic solar wall under tropical climate." M Eng. thesis Energy Technology Program, King Mongkut's University of Technology, Thornburi.

Kruger, E. (2008). "Thermal monitoring and indoor temperature predictions in a passive solar building in an arid environment." Energy and Building 43 1792–1804.

Labs, K., Cook (Ed.), J. (1989). "Passive Cooling." MIT Press, Cambridge, Massachusetts.

Laustsen, J. (2008). "Energy efficiency requirements in building codes, energy efficiency policies for new buildings." International Energy Agency 85.

Ong, K. S., Chow, C. C. (2003). "Performance of a solar chimney." Solar Energy 74, 1-17.

Peretti, C., Zarrella, A., De Carli, M., Zecchin, R. (2013). "The design and environmental evaluation of earth to-air heat exchangers (EAHE)." A literature review. Renew Sustain Energy Rev 28:107–16.

Republic of Lebanon Ministry of Public Works and Transport (2005). "Energy Analysis and Economic Feasibility." UNDP/GEF, MPWT/DGU, p. 63.

Roodman, D. M., Lenssen, N. (1995). "World Watch Paper 124, A Building Revolution: How Ecology and Health Concerns Are Transforming Construction." Worldwatch Institute, Washington.

Schulz, T., Eicker, U. (2013). "Controlled natural ventilation for energy efficient buildings." Energy Build 56:221–32.

Spieler, A., Wagner, R., Beisel, S., Vajen, K. (2000). "Passive solar office building: first experiences and measurements." in: 4th ISES Europe Solar Congress.

Swinbank, W. C. (1963). "Long-wave radiation from clear skies." Q. J. R. Meteoro. Soc. 89:339.

Voss, K., Herkel, S., Pfafferott, J., Lohnert, G., Wagner, A. (2007). "Energy efficient office buildings with passive cooling – results and experiences from a research and demonstration programme." Solar Energy 81 (3) 424–434.

Wagner, R., Beisel, S., Spieler, A., Gerber, A., Vajen, K. (2000). "Measurement, modeling and simulation of an earth-to-air heat exchanger in Marburg (Germany)." in: 4th ISES Europe Solar Congress, 2000.

Wigginton, M., Harris, J. (2002). "Intelligent Skins." Architectural Press, London.

Xing, Y., Hewitt, N., Griffiths, P. (2011). "Zero carbon buildings refurbishment - a hierarchical pathway." Renewable Sustainable Energy Rev 15:3229-36.

Yaghoubi, M., Sabzevari, A. (1987). "Studies on simulations of passive solar buildings." Solar Wind Technol. 4, 337-346.

Yassine, B., Ghali, K., Ghaddar, N., Srour, I., Chehab, G. (2012). "A numerical modeling approach to evaluate efficient mechanical ventilation strategies." Energy and Buildings, 618-613.

Yassine, B., Ghali, K., Ghaddar, N., Chehab, G., Srour, I. (2014). "Effectiveness of the earth tube heat exchanger system coupled to a space model in achieving thermal comfort in rural areas." International Journal of Sustainable Energy, 33 (3), pp. 567-586.

Yuebin, Yu., Haorong, Li., Fuxin, Niu., Daihong, Yu. (2013). "Investigation of a coupled geothermal cooling system with earth tube and solar chimney." Applied Energy, 114, pp. 209-217.

Zhang, H., Arens, E., Huizenga, C., Han, T. (2010). "Thermal sensation and comfort models for non-uniform and transient environments: part I: local sensation of individual body parts." Building and Environments 45 (2) 380–388.